High resolution stable isotope and carbonate variability during the early Oligocene climate transition: Walvis Ridge (ODP Site 1263)

Christina R. Riesselman,[1] Robert B. Dunbar,[1] David A. Mucciarone,[1] and Saya S. Kitasei[2]

[1]Department of Geological and Environmental Sciences, Stanford University, Braun Hall Bldg 320, Stanford, CA 94305-2115, USA
  (criessel@pangea.stanford.edu, dunbar@stanford.edu, dam@pangea.stanford.edu)
[2]Earth Systems Program, School of Earth Sciences, Stanford University, Mitchell Building, Room 138, Stanford, CA 94305-2210, USA
  (skitasei@stanford.edu)

Abstract   The rapid global increase in benthic foraminiferal $\delta^{18}O$ in the early Oligocene (~33.6 Ma) has been taken to imply the first appearance of large, permanent ice sheets on Antarctica, possibly coupled to deep sea cooling and/or Northern Hemisphere ice growth. This oxygen isotope shift is accompanied by a reorganization of the global carbon cycle, identified by a $\delta^{13}C$ increase that slightly lags the glacially-mediated $\delta^{18}O$ transition. Here, we present a new record of the early Oligocene climate transition from the subtropical South Atlantic Ocean. To investigate climatic and carbon cycle variability in the transition from the early Paleogene "greenhouse" into the Oligocene "icehouse" world, we have developed carbonate content, coarse fraction, and benthic foraminiferal carbon and oxygen stable isotope records for the earliest Oligocene at Ocean Drilling Program (ODP) Site 1263. These records represent the highest-resolution reconstruction of the Eocene/Oligocene from the Atlantic basin to date, and provide us with a unique opportunity to investigate the fine-scale interplay of glaciation and the global carbon cycle.

Introduction

Punctuated by the rapid development of permanent Antarctic ice sheets, the unidirectional transition from early Eocene "greenhouse" to early Oligocene "icehouse" is the most fundamental reorganization of global climate in the Cenozoic. Both coupled general circulation model investigations (e.g. DeConto and Pollard, 2003) and recent reconstructions of atmospheric carbon dioxide concentrations (Pagani et al., 2005) implicate climate sensitivity to declining $p\mathrm{CO_2}$ as a crucial factor in pushing the planet across a threshold into a state of permanent glaciation from which it has not since returned.

The $\delta^{18}O$ composition of benthic foraminifera is sensitive to both global ice volume and deep sea temperature. Existing marine records from the Atlantic, Pacific, and Southern oceans consistently document a >1‰ increase in $\delta^{18}O$ across the Eocene/Oligocene (E/O) transition (Coxall et al., 2005; Zachos et al., 1996). While the majority of this isotopic enrichment has been attributed to the initiation of major, continent-scale glaciation on Antarctica, the magnitude of the excursion is too large to result from ice growth alone. Although Mg/Ca-based temperature reconstructions have not identified benthic cooling concurrent with this major increase in Antarctic glaciation (Lear et al., 2000), some degree of deep cooling and/or ice growth in the Northern Hemisphere must be invoked to account for the full $\delta^{18}O$ excursion (Coxall et al.,2005; Eldrett et al., 2007). Refining our understanding of the nature of this transition as well as its influence on the carbon cycle sheds critical light on the complex interactions inherent in our climate system.

Leg 208, Site 1263

ODP Leg 208 recovered the E/O transition at five subtropical South Atlantic sites on the northwest flank of Walvis Ridge along a 2 km depth transect. Shipboard measurements of optical lightness (L*) and magnetic susceptibility at the deepest sites (Site 1262, 4755 m; Site 1267, 4355 m) mark the distinct and rapid transition from brown clay to carbonate-rich sediment that accompanies a sudden deepening of the calcite compensation depth (CCD) and increase in carbonate preservation in the early Oligocene (Zachos et al., 2004; Liu et al., 2004; Coxall et al., 2005). At the shallower sites (Site 1263, 2717 m; Site 1265, 3060 m), the transition from clay-bearing to carbonate sediment occurs gradually and reflects the position of these sites well above the lysocline in the latest Eocene. These shipboard physical properties measurements place the lysocline between sites 1267 and 1266 (3798 m) prior to the CCD deepening.

Situated at the cusp of the Walvis Ridge and well above the latest Eocene lysocline, Site 1263 (28°31.98'S, 2°46.77'E; 2100 m E/O paleodepth) recovered an E/O section unaffected by dissolution and reworking, with high mass accumulation rates (> 2x Site 1265 MAR) and linear sedimentation rates of ~15 m/m.y. (Zachos et al., 2004). As a result, Site 1263 provides the highest resolution Atlantic sequence to date for investigating the influence of orbital pacing on the initial Oligocene glaciation (Oi-1) event and attendant changes in the global carbon cycle.

Materials and methods

The Eocene/Oligocene transition interval at Site 1263 was recovered by Advanced Piston Coring (APC) from two holes offset from each other by ~20 m. Holes 1263A and 1263B were aligned based on magnetic susceptibility

profiles and representative sections were depth-shifted and spliced to obtain a composite section with 100% recovery; where reported, meters composite depth (mcd) is derived from this composite shipboard splice (Zachos et al., 2004).

Ten-cc samples were collected at 5 cm intervals from the shipboard splice spanning latest Eocene and early Oligocene times. Following the shipboard age model of Zachos et al. (2004), each 2-cm wide sample amalgamates between 1.6 and 2.4 kyr of accumulation with an average sampling interval of ~5 kyr. This sample spacing is the minimum interval sufficient to resolve the influence of the 19- and 23-kyr precessional cycles on ice volume, benthic temperature, and carbon cycle fluctuations.

Age model

The very soft nannofossil ooze at Site 1263 does not preserve a clean magnetic signal, precluding the development of a well-constrained paleomagnetic stratigraphy. As a result, significant post-cruise refinements have not been made to the Site 1263 age control. Using the seven age/depth points comprising the shipboard chronology for the latest Eocene and earliest Oligocene, we have applied a second-order polynomial regression to generate our age model (Fig. 1). These age control points result from interpolation between calcareous nannofossil and planktonic foraminifer datums and a partial resolution of the C13n magnetochron. Calcareous nannofossil biostratigraphy follows the mid- to low latitude nannofossil assemblage zonal scheme of Bukry (1973, 1975) with additional CN and CP zonal code notation after Okada and Bukry (1980). The planktonic foraminiferal zonal scheme follows Berggren et al. (1995). Magnetostratigraphic chron boundary ages follow Cande and Kent (1995). (See Shipboard Scientific Party, 2004 for additional information on shipboard biostratigraphy, magneto-stratigraphy, and age model development.)
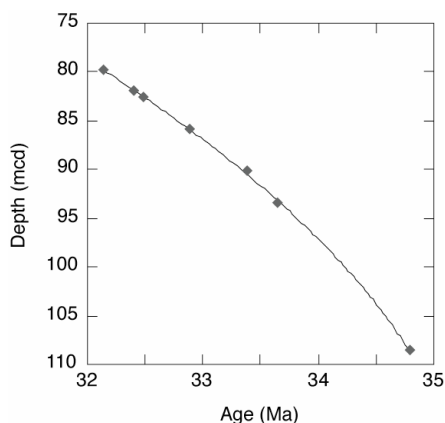

Figure 1. Site 1263 age model, based on Zachos et al. (2004) age control.

Because the age model is largely reliant on biostratigraphy, Site 1263 has a less robust chronology than high-resolution E/O isotope reconstructions with orbitally tuned age models (i.e. Coxall et al., 2005). Duration- and rate-dependent relationships are presented within this framework, and while age-based observations should be considered relative rather than absolute, they are nevertheless internally robust.

Coarse fraction and wt. % $CaCO_3$ determination

Approximately 10 g of wet sample was disaggregated in a 1% solution of sodium hexametaphosphate and deionized water buffered to pH ~9.5 with NH_3OH, then wet-sieved over a 63-μm sieve. Coarse and fine fractions were collected, dried in a hood, and weighed. Wt% sand fraction was calculated by dividing coarse fraction weight by the combined weight of coarse and fine fractions.

Most high-precision carbonate analyses of dried, homogenized bulk sediments were performed using a UIC Inc. Coulometrics Model 5011 CO_2 coulometer coupled to a Model CM5130 acidification module. For each analysis, 3-5 mg of dry crushed sediment was reacted in 3 ml of hot 12% phosphoric acid, using grade 4.8 N_2 carrier gas at a flow rate of 80-100 ml/minute. A small number of analyses were performed using a UIC Inc. Coulometrics Model CM5014 coulometer coupled to a Model CM5240 TIC autoanalyzer. Method precision using the manual acidification module is generally better than ±0.2%, although a small number of replicate values differ by up to 0.6%. Inter-method precision on this suite of samples is better than ±0.8%.

$\delta^{18}O$ and $\delta^{13}C$ analysis

In order to assess the variable influence of dissolution, reworking, and downslope transport on different benthic species, duplicate oxygen and carbon isotope analyses were performed on size-grouped specimens of *Oridorsalis umbonatus*, *Cibicidoides praemundulus*, *C. havanensis*, *C. grimsdalei*, and *Nuttallides trumpeyi* from five Site 1263 corecatcher samples spanning 40 meters (79-117 mcd) across the E/O climate transition. Of these species, *O. umbonatus* was present at all depths and had the narrowest range of variability, with maximum standard deviations for $\delta^{18}O$ and $\delta^{13}C$ of 0.21‰ and 0.22‰ respectively. A significant portion of this variability was associated with specimens >300μm or <125μm, while small and medium sized individuals (125-250μm) generated the most reproducible values. Excluding large and very small individuals from analysis improved oxygen isotope standard deviations to better than 0.12‰ at all depths and carbon isotope standard deviations to better than 0.14‰. By comparison, average standard deviations for *Cibicidoides* $\delta^{18}O$ within a narrow size range were greater than 0.25‰.

Based on these results, *O. umbonatus* was selected for all isotope analyses reported here. In order to determine

average composition, most samples combine between 5 and 9 individuals distributed across the 125-250 μm size range. Specimens were cleaned of surface contamination with deionized water and crushed inside a Kiel reaction vial in preparation for analysis in the Stanford University Stable Isotope Laboratory. Benthic foraminiferal carbonate was reacted with anhydrous phosphoric acid at 70° C in an automated Kiel III carbonate device coupled to a Finnigan MAT 252 isotope ratio mass spectrometer. Instrument voltage is determined by sample mass; where reported, isotopic averages for replicate analyses have been weighted by voltage to more accurately represent sample composition. Standard deviation of the NBS-19 isotopic reference material analyzed with each suite of samples documents instrumental precision of 0.03‰ for $\delta^{13}C$ and better than 0.06‰ for $\delta^{18}O$. Stable isotope data are reported in per mil (‰) notation, relative to the Vienna PeeDee Belemnite (VPDB) standard and have not been normalized to equilibrium sea water values.

Cibicidoides spp. have been the common currency for reconstruction of Cenozoic climate trends and events (e.g. Zachos et. al., 2001). However, Katz et al. (2003) identify the potential of *Oridorsalis* spp. to "provide the most reliable deepwater isotopic recorder" of early Paleogene extreme climate events because 1) *Oridorsalis* persists across the extinctions of other taxa commonly used for isotope reconstructions; 2) *Oridorsalis* increases in abundance in the early Eocene across the Atlantic and in parts of the Pacific; 3) *Oridorsalis* calcite records equilibrium $\delta^{18}O_{seawater}$ values in the modern ocean; and 4) *Oridorsalis* offers good paired analysis linearity to both *Cibicidoides* and *N. trumpeyi*, allowing the development of reliable correction factors to normalize between species and records. At Site 1263, a small number of paired analyses of *O. tener* and *O. umbonatus* showed good reproducibility (maximum standard deviation of 0.14‰ for both $\delta^{18}O$ and $\delta^{13}C$), additionally suggesting a consistent vital effect across Oligocene *Oridorsalis* species.

Statistical analysis of $\delta^{13}C$, and $CaCO_3$ time series

Visual inspection of the $CaCO_3$ and $\delta^{13}C$ time series suggests the presence of periodic variability following the establishment of post-Oi-1 "stable" Oligocene glaciation. Frequency domain time series analysis included both multi-taper method (MTM) power spectra and wavelet spectra to identify the significant frequencies present and how they vary in time. We found that using a resampled time series with a constant time step of 3.5 kyr minimized leakage of spectral energy into harmonics while preserving the variance in the power spectrum. To facilitate comparison between the frequency domain analyses of the $\delta^{13}C$ and $CaCO_3$ time series, we converted each series to units of

standard deviation (std units). Both series display long-term non-periodic variations on time scales longer than 200 kyr; in order to focus on and isolate the orbital scale variability, we calculated and subtracted the first three reconstructed Singular Spectrum Analysis (SSA) components from the normalized time series using the SSA Toolkit (Ghil et al., 2002; Dettinger et al., 1995) and recalculated the MTM power spectra. Wavelet power spectra (Torrence and Compo, 1998) were calculated for both normalized and differenced time series, using a Morlet wavelet and a lag-1 autocorrelation coefficient of 0.53 for $CaCO_3$ and 0.35 for $\delta^{13}C$.

Results

Benthic $\delta^{18}O$ and $\delta^{13}C$, weight % $CaCO_3$, % sand (>63 μm), and magnetic susceptibility measurements are plotted against meters composite depth (mcd) for the early Oligocene interval of the Site 1263 multi-hole splice (Fig. 2). Agreement between the Site 1263 $\delta^{18}O$ profile and 1) earlier benthic oxygen stable isotope reconstructions from Site 522 in the Atlantic and Site 744 in the Indian sector of the Southern Ocean, and 2) the global compilation of Zachos et al. (2001) suggests that Site 1263 preserves the interval at high resolution, from the ice-free earliest Oligocene through the Oi-1 transient into a moderate stable Oligocene glacial state. However, the high-resolution Site 1263 record does not reproduce the stepwise character of the transition recently identified from Site 1218 in the tropical Pacific (Coxall et al., 2005).

$\delta^{18}O$ and $\delta^{13}C$

Site 1263 provides the highest-resolution Atlantic $\delta^{18}O$ record to date of the benthic isotopic record of the onset of Oligocene glaciation on Antarctica, and can be separated into three intervals. Prior to the initiation of continent-scale ice sheets, $\delta^{18}O$ variability is low, with an average pre-glacial value of 1.4‰. Starting at 94.49 mcd, $\delta^{18}O$ increases to an Oi-1 maximum of ~2.6‰ over ~1.3 m, but like others from the Atlantic, the record at this site does not show the two shifts in $\delta^{18}O$ characteristic of the stepwise onset of Antarctic glaciation and contemporaneous benthic cooling in the Pacific (Coxall et al., 2005). In addition, the Site 1263 $\delta^{18}O$ record exhibits significant high-magnitude variability during the Oi-1 interval that has not previously been observed. Following the transition into Oi-1, $\delta^{18}O$ values remain high for ~4.4 m, to 88.79 mcd. It is not possible to distinguish Oi-1a and Oi-1b, the two discrete peaks commonly identified in early Oligocene isotope reconstructions (e.g. Zachos et al., 1996) including Leg 208 site 1262 (Liu et al., 2004). After the Oi-1 isotope maximum, $\delta^{18}O$ settles to more "stable" glacial average values of ~2.2‰. $\delta^{13}C$ also increases significantly across the Oi-1 transition. From an average value of 0.2‰ at the base of the record, $\delta^{13}C$ increases only slightly to ~0.3‰ at 94.44 mcd and at 93.09 mcd rapidly increases by 0.9‰, reaching a transitory maximum of ~1.2‰ at 92.69 mcd.
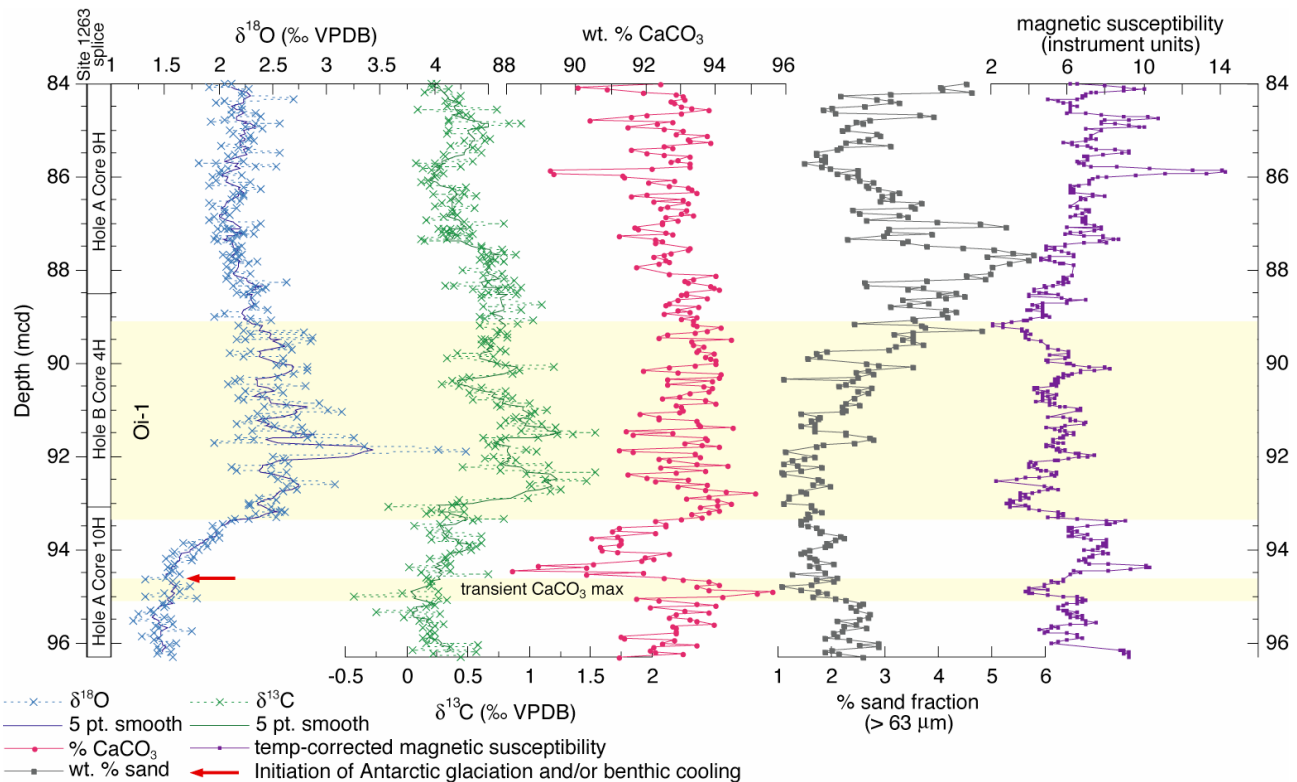
Figure 2. Benthic foraminifer stable isotope data, wt % CaCO3, % sand fraction, and shipboard magnetic susceptibility from the Site 1263 shipboard composite stratigraphic splice, plotted against meters composite depth. All replicate *Oridorsalis umbonatus* data plotted as x's. Narrow yellow envelope (~95 mcd) encompasses a transient % $CaCO_3$ maximum prior to the initiation of the Oligocene glacial interval (see text); broad yellow envelope (~89-93) encompasses the Oi-1 interval at this site.

CaCO₃ content, sand fraction, and magnetic susceptibility

The wt. % $CaCO_3$ record at Site 1263 extends below the base of the benthic foraminiferal isotope record (Fig. 3A). Bulk sediment wt. % $CaCO_3$ fluctuates around ~93% for much of the record. One notable feature in the carbonate profile is a transient 20 cm increase at 95.04 mcd (to a maximum of ~96%), just prior to the initiation of the Oi-1 $\delta^{18}O$ excursion, accompanied by decreases in percent sand fraction and magnetic susceptibility (Fig. 2). This abrupt increase is followed immediately by a decrease to a minimum of ~88% at 94.44 mcd, with a second pulse of low $CaCO_3$ (~90.5%) at 93.74 mcd. Both of these low carbonate pulses are accompanied by increases in magnetic susceptibility, and are restricted in duration to the $\delta^{18}O$ transition interval (Fig. 2).

The Site 1263 percent sand fraction (% >63 μm by weight) is composed primarily of planktonic foraminifera, with a secondary contribution from benthic foraminifera; fine fraction is overwhelmingly composed of calcareous nannofossils. Coarse fraction concentrations at the base of the isotope record are greater than 2%, decreasing gradually to ~1% around 92.99 mcd, then increasing to a section maximum of nearly 6% at 87.67 mcd. Following this maximum, concentrations decrease again to ~1.5% at 85.72 mcd before increasing to ~4.5% at the top of the isotope record. The Site 1263 coarse fraction record reproduces the structure of the sand fraction profile from nearby abyssal Site 522 (Angola Basin) to a surprising degree, suggesting regional rather than local control.

Discussion

The transition from Eocene "greenhouse" conditions into Oligocene glaciation is the most fundamental reorganization of the global climate system in the Cenozoic (Zachos et al., 2001). The $\delta^{18}O$, $\delta^{13}C$, wt. % $CaCO_3$, and % sand records developed from the early Oligocene section at Site 1263 are the first records from the Atlantic with sufficiently high resolution to examine the detailed relationships between the initiation of Antarctic glaciation, circulation, and the global carbon cycle.

A brief but pronounced increase in wt. % $CaCO_3$ directly precedes the initiation of ice growth as recorded in Site 1263 $\delta^{18}O$; this transient maximum is immediately followed by a rapid reversal into an interval of low carbonate concentration (Fig. 3B). Although a unidirectional increase in % $CaCO_3$ accompanies the initiation of glacial conditions at most Leg 208 sites (Liu et al., 2004; Zachos et al., 2004), carbonate content at Site 1263 remains below the background average for the duration of the transition into Oi-1. Because carbonate
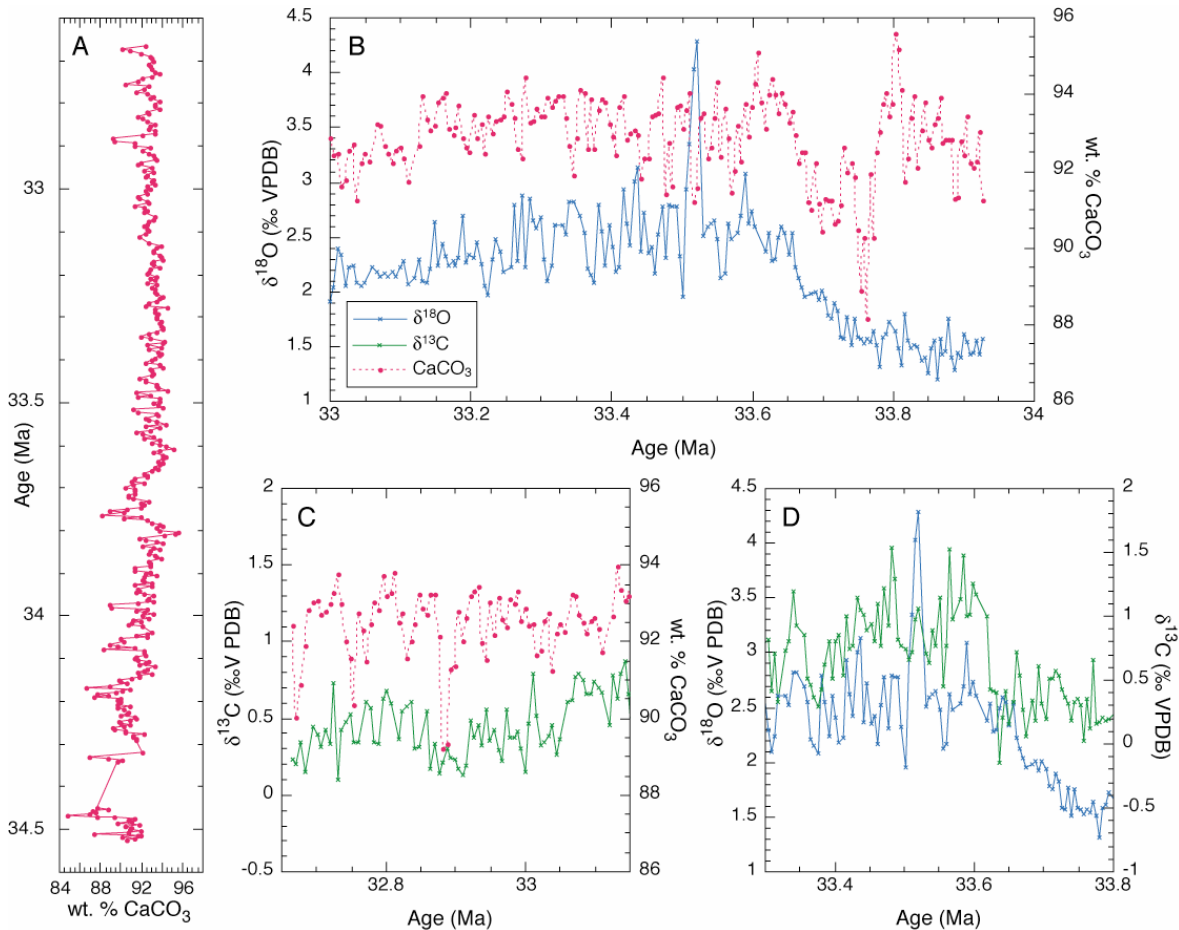
4

Figure 3. Selected Site 1263 intervals; replicate isotope analyses are voltage-weighted and plotted as a single point average. A.) Extended record of wt. % $CaCO_3$. B.) $\delta^{18}O$ (blue x's, left axis) versus $CaCO_3$ (pink circles, right axis) for the interval from 34 – 33 Ma, demonstrating the phasing of the transient $CaCO_3$ maximum and subsequent decline relative to the early Oligocene oxygen isotope excursion. C.) $\delta^{13}C$ (green x's, left axis) versus $CaCO_3$ (pink circles, right axis) for the 500 kyr interval from 33.15 – 32.65 Ma, highlighting contrasting periods of variability. D.) $\delta^{18}O$ (blue x's, left axis) versus $\delta^{13}C$ (green x's, right axis) for the 500 kyr interval from 33.8 – 33.3 Ma, highlighting the lag between the carbon and oxygen isotope excursions.

accumulation is sensitive to a variety of local factors such as surface productivity, dissolution, and dilution by non-carbonate sediment, this pre-glaciation transient carbonate maximum likely represents a local signal. However a moderate-resolution % $CaCO_3$ record from Kerguelen Plateau Site 744, which has similar E/O paleodepth to Site 1263, exhibits a similar increase immediately prior to the interval of enhanced biogenic opal accumulation that accompanies the initiation of glaciation (Salamy and Zachos, 1999). Many existing % $CaCO_3$ records from E/O ODP and DSDP material are not of sufficient resolution to identify the presence or absence of a similar event, but it may be worthwhile to seek an appropriate shallow, high-resolution Pacific section and to calculate carbonate mass accumulation rates to further investigate the possible extent of this transient.

$\delta^{18}O$ at the Oi-1 transition records a gradual onset of Antarctic glaciation followed by a rapid acceleration of ice growth and subsequent relaxation into a more stable state. In fact, this first Oligocene glacial event, characterized as an overshoot of Antarctic ice growth beyond a glacial equilibrium climate state and into an extreme state of unusually deep glaciation, may have been characterized by near-present day Antarctic ice volume (Coxall et al., 2005; Zachos and Kump, 2005). Based on the shipboard age model, the gradual $\delta^{18}O$ increase at Site 1263 begins around 33.77 Ma (Fig. 3B). The initial phase of the transition takes place at a moderate pace, with about 0.5‰ of the total 1.2‰ increase occurring over approximately 100 kyr. The rate of increase (and by association, the rate of glaciation) then accelerates significantly, so that the later 0.7‰ of the transition occurs within less than 30 kyr. The pattern of ice accumulation inferred by this two-part transition supports the hypothesis that hysteresis associated with ice-sheet height mass balance feedbacks, in combination with declining pCO_2 and high-frequency orbital variability,

influences the pacing of Oligocene ice growth (Pollard and DeConto, 2005).

The Site 1263 benthic $\delta^{18}O$ profile nicely reproduces earlier Atlantic and South Indian transition interval reconstructions (e.g. Zachos et. al., 1996), however all of these differ significantly from the very high resolution tropical Pacific record from Site 1218 (Coxall et al., 2005). A possible explanation for this difference may involve the onset of North Atlantic Deep Water (NADW) formation in the early Oligocene (Davies et al., 2001). A recent Nd isotope reconstruction of deep-water mass evolution by Via and Thomas (2006) places the arrival of NADW at Walvis Ridge around 33 Ma. Presumably, such a fundamental change in deep-water circulation disturbed the global circulation balance and influenced the various ocean basins in different ways. Additional water-mass reconstructions of the E/O transition interval at higher resolution will be required to address this open question.

The $\delta^{13}C$ transition lags the $\delta^{18}O$ transition across the early Oligocene transition interval, suggesting a causal relationship between $\delta^{18}O$ and $\delta^{13}C$ increases. At most E/O sites this lag is relatively brief: ~20kyr at abyssal Atlantic Site 522 and shallow Southern Ocean site 744 (Salamy and Zachos, 1999; Zachos and Kump, 2005), and <10 kyr at Equatorial Pacific site 1218 (Coxall et al., 2005). At Site 1263, however, this lag is significantly longer. In this section, Oi-1 glaciation appears to be fully established before the initiation of ^{13}C enrichment, suggesting a lag of >90 kyr between initiation of $\delta^{18}O$ and $\delta^{13}C$ increases. This disparity between our record and other established reconstructions may result in part from uncertainty in our age model. However, an additional explanation will be necessary to reconcile such a significant difference. It is possible, for instance, that a unique intermediate water mass buffered Site 1263 from the global carbon isotopic increase during the transition, although current reconstructions are not of sufficient resolution to test this hypothesis.

Following the extreme, transient Oi-1 glaciation, Oligocene climate settled into a more moderate and stable glacial mode. Site 1263 $\delta^{13}C$ is periodically variable across the unstable Oi-1 overshoot, implying orbital pacing. Furthermore, distinct periods of variance in $CaCO_3$ and $\delta^{13}C$ in the stable Oligocene glacial interval following Oi-1 (Fig. 2C) are evident by visual inspection, with higher-frequency periodicity in the $\delta^{13}C$ record and lower- frequency periodicity in the $CaCO_3$ record. The limits of our age model preclude decisive assignment of orbital periodicities to the observed variability, but comparison of wavelet spectra for $\delta^{13}C$ and $CaCO_3$ (Fig. 4) identifies primary features that may reflect orbital variability. In the carbon isotope record; two intervals of high frequency (~30 kyr) variability centered around 33 Ma exceed the 95% significance level and are also identifiable in the normalized time series; a third lower-frequency interval spans the Oi-1. The carbonate time series exhibits two discontinuous intervals of lower-
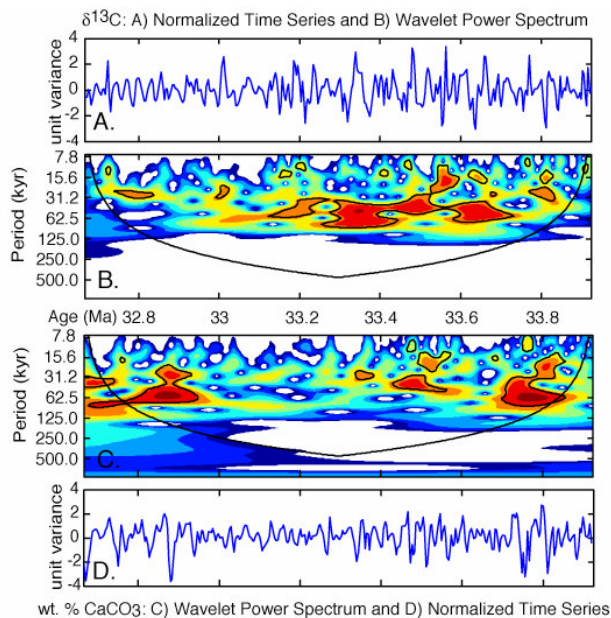

Figure 4. Wt. % $CaCO_3$ and $\delta^{13}C$ time series and calculated wavelet power spectra. A.) $\delta^{13}C$ time series, sampled at 3500 yrs and normalized to unit variance. B.) $\delta^{13}C$ continuous wavelet transform, calculated using a Morlet wavelet from an algorithm by Torrence and Compo (1999). Variance is plotted as a function of both time and period; the heavy dark line surrounds regions of variance that exceed the 95% confidence level for a red noise (AR1) process using a lag-1 autocorrelation of 0.35. The convex curve at the base of the plot outlines the cone of influence; variance plotted below this line has been reduced due to the wavelet reaching the end of the finite time series. C.) $CaCO_3$ continuous wavelet transform, calculated as above using a lag-1 autocorrelation of 0.53. D.) CaCO3 time series, sampled at 3500 yrs and normalized to unit variance.

frequency variance at ~50 kyr. The first is centered at 33.8 Ma and the second at 32.8 Ma; there is very little coherence in the $CaCO_3$ record in the interval spanning the primary Oi-1 transition and intense glaciation.

It is clear that these two records are responding to different periodic forcing mechanisms during the early Oligocene. Numerous records identify enhanced Southern Ocean primary productivity accompanying the development of a stable Oligocene Antarctic Ice Sheet (e.g. Diester-Haas, 1995; Nilsen et al., 2003). We propose that longer-frequency variations in $CaCO_3$ content reflect local accumulation and dissolution processes, while the cyclic variations in carbon isotopes record the development of a high-latitude productivity regime at the heart of the Oligocene global carbon cycle.We further suggest that the apparent 30 kyr and 50 kyr variance periods in carbon isotopes and %$CaCO_3$ respectively may in fact be representative of the 21 or 23 kyr precessional and 41 kyr obliquity signals. Tuning Site 1263 to these orbital frequencies would compress the age model by

~25%, correcting a portion of the anomalously long lag between the Oi-1 $\delta^{18}O$ and $\delta^{13}C$ transitions and facilitating further comparison between Site 1263 and other E/O climate records.

Summary

Site 1263 provides the highest-resolution record of the E/O climate transition from the Atlantic Ocean to date. The $\delta^{18}O$ of *O. umbonatus* at Site 1263 faithfully reproduces the structure identified at other Atlantic sites but differs from Pacific Site 1218, perhaps suggesting the variable influence of changes in deep water-mass circulation. The pattern of ice accumulation inferred by the gradual-to-rapid transition into Oi-1 supports the influence of hysteresis in the pacing of Oligocene ice growth. Clearly, Atlantic and Pacific high-resolution reconstructions of circulation, in addition to temperature and ice volume, will be necessary to further constrain potential forcings and responses during this important interval of global reorganization.

References

Berggren, W.A., D.V. Kent, C.C Swisher III, and M.-P Aubry (1995), A revised Cenozoic geochronology and chronostratigraphy. *in* Berggren, W.A., Kent, D.V., Aubry, M.-P., and Hardenbol, J. (Eds.), Geochronology, Time Scales and Global Stratigraphic Correlation, Spec. Publ. - SEPM (Soc. Sediment. Geol.), 54:129–212.

Bukry, D. (1973), Low-latitude coccolith biostratigraphic zonation, *in* Edgar, N.T., J.B. Saunders, et al., Init. Repts. DSDP, 15: Washington (U.S. Govt. Printing Office), 685–703.

————, (1975), Coccolith and silicoflagellate stratigraphy, northwestern Pacific Ocean, Deep Sea Drilling Project Leg 32. *In* Larson, R.L., R. Moberly, et al., Init. Repts. DSDP, 32: Washington (U.S. Govt. Printing Office), 677–701.

Cande, S.C., and D.V. Kent (1995). Revised calibration of the geomagnetic polarity timescale for the Late Cretaceous and Cenozoic, J. Geophys. Res*.*, 100, 6093–6095.

Coxall, H.K., P.A. Wilson, H. Pälike, C.H. Lear, and J. Backman (2005), Rapid stepwise onset of Antarctic glaciation and deeper calcite compensation in the Pacific ocean, Nature, 433, 53-57.

Davies. R., J. Cartwright, J. Pike, and C. Line (2001), Early Oligocene initiation of North Atlantic Deep Water formation, Nature, 410, 917-920.

DeConto, R.M and D. Pollard (2003), Rapid Cenozoic glaciation of Antarctica induced by declining atmospheric CO_2, Nature, 421, 245-249.

Dettinger, M.D., M. Ghil, C.M. Strong, W. Weibel, and P. Yiou (1995), Software expedites singular-spectrum analysis of noisy time series, Eos, Trans. Am. Geophys. Union, 76(2), 12,14,21.

Diester-Haass, L. (1995) Middle Eocene to early Oligocene paleoceanography of the Antarctic Ocean (Maud Rise, ODP Leg 113, Site 689): change from a low to a high productivity ocean, Palaeogeogr. Palaeoclimatol, Palaeoecol., 113, 311-334.

Eldrett, J.S., I.C. Harding, P.A. Wilson, E. Butler, and A.P. Roberts (2007), Continental ice in Greenland during the Eocene and Oligocene, Nature, 446, 176-179.

Ghil, M., R.M. Allen, M.D. Dettinger, K. Ide, D. Kondrashov, M.E. Mann, A. Robertson, A. Saunders, Y. Tian, F. Varadi, and P. Yiou (2002), Advanced spectral methods for climatic time series, Rev. Geophys., 40(1), 3.1-3.41.

Katz, M.E., D.R. Katz, J.D. Wright, K.G. Miller, D.K. Pak, N.J. Shackleton, and E. Thomas (2003), Early Cenozoic benthic foraminiferal isotopes: Species reliability and interspecies correction factors, Paleoceanography, 18(2): 2.1-2.12.

Lear, C.H., H. Elderfield, and P.A. Wilson (2000), Cenozoic deep-sea temperatures and global ice volumes from Mg/Ca in benthic foraminiferal calcite, Science, 287, 269-272.

Liu, Z., S. Tuo, Q. Zhao, X. Cheng, W. Huang (2004), Deep-water Earliest Oligocene Glacial Maximum (EOGM), South Atlantic, Chin. Sci. Bull., 49(20), 2190-2197.

Nilsen, E.B., L.D. Anderson, and M.L. Delaney (2003), Paleoproductivity, nutrient burial, climate change and the carbon cycle in the western equatorial Atlantic across the Eocene/Oligocene boundary, Paleoceanography, 18(3), 2-1–2-11.

Okada, H., and D. Bukry (1980), Supplementary modification and introduction of code numbers to the low-latitude coccolith biostratigraphic zonation (Bukry, 1973; 1975), Mar. Micropaleontol., 5, 321–325.

Pagani, M., J.C. Zachos, K.H. Freeman, B. Tipple, S. Bohaty (2005), Marked decline in atmospheric carbon dioxide concentrations during the Paleogene, Science, 309, 600-603.

Pollard, D. and R.M. DeConto (2005), Hysteresis in Cenozoic Antarctic ice-sheet variations, Global Planet. Change, 45, 9-21.

Salamy, K.A. and J.C. Zachos (1999), Latest Eocene-Early Oligocene climate change and Southern Ocean fertility: inferences from sediment accumulation and stable isotope data, Palaeogeogr. Palaeoclimatol, Palaeoecol., 145, 61-77.

Shipboard Scientific Party (2004), Explanatory Notes, *in* Zachos, J.C., D. Kroon, P. Blum, et al., Proc. ODP, Init. Repts., 208, 1-63 [CD-ROM]. Available from: Ocean Drilling Program, Texas A&M University, College Station TX 77845-9547, USA.

Torrence, C. and G.P. Compo (1998), A practical guide to wavelet analysis, Bull. Amer. Meteor. Soc., 79, 61-78.

Tripati, A., J. Backman, H. Elderfield, and P. Feretti (2005), Eocene bipolar glaciation associated with global carbon cycle changes, Nature, 436, 341-346.

Via, R.K. and D.J. Thomas (2006), Evolution of Atlantic thermohaline circulation: Early Oligocene onset of deep-water production in the North Atlantic, Geology, 34(6), 441-444.

Zachos, J.C., D. Kroon, P. Blum, et al. (2004), Proc. ODP, Init. Repts., 208 [CD-ROM]. Available from: Ocean Drilling Program, Texas A&M University, College Station TX 77845-9547, USA

Zachos, J.C. and L.R. Kump (2005), Carbon cycle feedbacks and the initiation of Antarctic glaciation in the earliest Oligocene, Global Planet. Change 47, 51-66.

Zachos, J.C., M. Pagani, L. Sloan, E. Thomas, and K Billups (2001), Trends, rhythms, and aberrations in global climate 65 Ma to present, Science*,* 292, 686–693.

Zachos, J.C., T.M. Quinn, K. and Salamy (1996), Earliest Oligocene climate transition: constraints from high resolution (104 yr) deep-sea foraminiferal 18O and 13C time-series, Paleoceanography*,* 21, 251–266